Talanta 213 (2020) 120779

Contents lists available at ScienceDirect

Talanta

journal homepage: www.elsevier.com/locate/talanta

A novel ultrasensitive immunosensor based on disposable graphite paper electrodes for troponin T detection in cardiovascular disease

Burçak Demirbakan*, Mustafa Kemal Sezgintürk

Çanakkale Onsekiz Mart University, Faculty of Engineering, Bioengineering Department, Çanakkale, Turkey

ARTICLE INFO

Keywords:
Graphite paper (GP)
Troponin T (TnT)
Biosensor
Single frequency impedance (SFI) technique

ABSTRACT

Troponin T, which is a biomarker of cardiovascular disease, is vital for acute myocardial infarction (AMI). AMI is the most well-known cause of death in the world. In the present work, we designed a novel immunosensor using disposable, cheap, and very conductive graphite paper electrodes (GP). The proposed immunosensor was modified with hydrochloric acid (HCl) for immobilization of anti-TnT antibody. After carboxyl group formation on the surface, the GP electrodes were incubated with EDC/NHS pair as a cross-linker. Electrochemical impedance spectroscopy (EIS), single frequency impedance (SFI), cyclic voltammetry (CV) and square wave voltammetry (SWV) techniques were used for electrochemical characterization of the label-free immunosensor. Furthermore, the fabrication process of the proposed immunosensor was examined by using scanning electron microscopy (SEM). The proposed electrochemical immunosensor had a wide detection range (0.5 fg - 1000 fg/mL), and low limit of detection (LOD) and low limit of quantification (LOQ) at 1.28 fg/mL and 4.29 fg/mL, respectively. The designed immunosensor exhibited very good sensitivity, reproducibility, repeatability, reusability and long storage life. Additionally, the immunosensor was successfully applied to detection of TnT in human serum.

1. Introduction

Cardiovascular diseases (CVD), which have been increasing in recent years and threaten human health considerably, are at the top of the list of chronic diseases in the world [1]. The early diagnosis of cardiovascular diseases has undoubtedly become a very important need for human health, as they affect the mortality rate on a global scale and can progress in many people in daily life without a long-term presence in the body despite very serious damaging effects.

Cardiac troponin T (cTnT) and cardiac troponin I (cTnI) are more sensitive and specific than other cardiac biomarkers, i.e. myoglobin and creatine-kinase MB for acute myocardial infarction (AMI) [2]. Both are released within 2–4 h and 3–4 h after death cell, respectively, after the onset of AMI symptoms [3]. Some results are favorable for cTnI [4]. However, a comparison was made between sensitive cTnT and highly sensitive cTnI [5]. In principle, cTnT and cTnI remain in the bloodstream for more than 10 days, reaching a peak about 1–2 days after myocardial damage [6]. These biomarkers are useful in diagnosing acute myocardial infarction due to prolonged release in the blood [2]. Because cardiac troponin is a cardiac-specific biomarker, it helps isolate cardiac injury from skeletal muscle or other organ damage [7].

The use of biosensors for early detection of CVD has increased in recent years. This increase in biosensors is closely related to advantages such as enabling the precise determination of cost effective, bioactive species, and the ability to be designed with high selectivity. The basic principle of biosensors is based on the ability of the bioactive species to analyze the change in the environment in the presence of a transducer. Thus, alternatives can be modified in many ways.

Biosensor systems are designed to identify biologically active species in the body, while biomarkers are specific or susceptible to any type of disease. These can be determined in samples taken from very small volumes of body fluids such as serum, cerebrospinal fluid (CSF) and saliva. Biosensors are not only very convenient for use in clinical applications, but also they can be designed with high precision and low cost.

In recent years, practical, novel materials have been preferred to develop the disposable sensor systems with cost-effective properties and highly sensitivity, such as indium tin oxide glass based electrode [8,9], and graphite paper (GP) based electrode [10,11], pencil graphite electrode [12,13]. GP electrode has also some advantages such as durableness, ultra conductive carbon surface for practical immobilization methods, cheapness, surface stability compared to the other working electrodes such as gold electrode or pencil graphite electrode used in many biosensors.

* Corresponding author.
E-mail addresses: burcakdemirbakan@comu.edu.tr (B. Demirbakan), msezginturk@comu.edu.tr (M. Kemal Sezgintürk).

https://doi.org/10.1016/j.talanta.2020.120779
Received 15 September 2019; Received in revised form 9 January 2020; Accepted 22 January 2020
Available online 23 January 2020
0039-9140/ © 2020 Elsevier B.V. All rights reserved.

Table 1
Comparison of analytical properties of various TnT biosensors reported in the literature.

Immobilization Method	Methods	Detection Range	LOD	Reference
Janus microparticle	Optic	10–10^5 pg/mL	50 pg/mL	[15]
Ferreosen mod. silica NP	SWV	24–2.4 × 10^5 pgmL	24 pg/mL	[16]
(QDs)/$Ti0_2$ NP	PEC	0.1–1 pg/mL	0.1 pg/mL	[17]
NAFD	Electrochemistry	0.1–100 pg/mL	10 fg/mL	[18]
Ag@SnO_2	Electrochemiluminescence	1-105 fg/mL	0.11 fg/mL	[19]
N-MIP graphene -based sensor	Electrochemistry	0.02–0.09 ng/mL	0.008 ng/mL	[20]
TRFIA	Time-resolved fluorometry	3.24–963.71 pg/mL	2.21 pgmL	[21]
Aptasensor	DPV	0.05–5.0 ng/mL	23 pg/mL	[22]
MIP/BNQDs/GCE	DPV	0.01–5.0 ng/mL	0.0005 ngmL	[23]
PMB/MWCNTs	Electrochemistry	0.10–8.0 pgmL	0.04 pg/mL	[24]
GP/HCl/A-TnT	EIS and CV	0.5–1000 fg/mL	1.28 fg/mL	

As can be seen from the results obtained from the regeneration study (Fig. 5A), this electrode had a very stable surface and allowed a stable and practical immobilization.

In this study, electrochemical impedance spectroscopy, cyclic voltammetry, square wave voltammetry, and single frequency technique were utilized for immobilization, optimization, and characterization studies during biosensor design. SEM was used to monitor the morphological changes of the surface during the immobilization step. The clinical potential of the proposed immunosensor was investigated by analyzing real serum samples with the standard addition method. It was observed that the biosensor system developed for detection of cardiovascular diseases has very high sensitivity, excellent reproducibility and reusability capacity, long shelf life and high sensitivity for the analysis of serum samples.

The analytical comparison of the designed biosensor with various TnT sensors reported in the literature is given in Table 1. When the TnT immunosensor is compared to other sensors in this table; it is clearly demonstrated that the designed biosensor is able to give a response to the lower TnT concentrations, presents wider linear range for TnT protein and has ultra-high sensitivity.

2. Material and methods

2.1. Chemicals and instruments

All chemicals (Hydrochloric acid (HCl, 37%), *N*-(3-Dimethylaminopropyl)-*N′*-ethylcarbodiimide (EDC), *N*-hydroxysuccinimide (NHS)), biorecognition materials (TnT antibody, TnT antigen and BSA (bovine serum albumin) protein) were purchased from Sigma-Aldrich (St. Louis, M.O., USA). Graphite paper (GP) sheets (thickness: 0.3 ± 0.01 mm, size: 210 mm × 210 mm, 3 mΩ/cm^2) were purchased from Xiamen Tob New Energy Technology (Co. Ltd, Fujian, China). Reference electrode and counter electrode were purchased from BASi (West Lafayette, IN, USA). The whole proteins were prepared by using a phosphate buffer (50 mM, pH 7.0) and kept at − 20 °C till used. Also, 5 mM $[Fe(CN)_6]^4$/5 mM $[Fe(CN)_6]^3$ (1:1) which is a redox probe solution containing 0.1 M KCl, was prepared with ultra-pure water. Using three - electrode system has an Ag/AgCl (saturated with KCl) as a reference electrode, a platinum wire as a counter electrode and except disposable GP electrode as a working electrode (5 mm × 20 mm, 3 mΩ/cm^2) in this study. Clinical human serum samples were obtained from the Çanakkale Onsekiz Mart University Hospital.

All electrochemical impedance, cyclic voltammetry and square wave voltammetry analyses were performed with Gamry Potentiostat/Galvanostat (Reference 600, Gamry Instruments, Warminster, PA, USA) connected with a computer via an EChem Analyst software throughout the entire study. PURELAB flex 3 & 4 Ultrapure Water Purification System (ELGA LC 134 model) was used during the all preparation stages of the proposed immunosensor for ultra-pure water. The surface morphologies of GP electrodes were examined through monitoring by a thermal field emission scanning electron microscope (JEOL JSM-7100 F model). The SEM measurements were carried out at the Science and Technology Application and Research Center of Çanakkale Onsekiz Mart University (ÇOBİLTUM). To obtain the SEM images, 5 kV was used as an acceleration voltage.

2.2. Fabrication of the TnT immunosensor

Firstly, disposable GP electrodes were cleaned in ethanol and ultrapure water (18.2 MΩ deionized) with the help of an ultrasonic bath for 5 min, respectively. After, the GP electrodes were treated with HCl acid solution (6.25 M) overnight in darkness for immobilization. Thereafter the HCl process, the EIS and CV measurements of the GP electrodes were taken and they were incubated in EDC/NHS (0.4 mM; 0.1 mM) which is prepared in the phosphate buffer (pH 7.0), for 1 h. Anti-TnT antibodies were immobilized on the electrode surface for 30 min. Then, the GP electrodes were immersed in BSA solution (blocking agent, 0.5%, w/v) for 1 h. After this step, the immobilization procedure of the TnT immunosensor was completed. Along the immobilization steps, GP electrodes were washed with ultra-pure water and were dried with argon gas at room temperature. The fabrication steps of the TnT immunosensor are presented in Scheme 1.

2.3. Electrochemical measurement for the TnT immunosensor

The electrochemical impedance spectroscopy and the cyclic voltammetry were utilized for all immobilization steps of the TnT immunosensor. The CV measurements were carried out in a potential range (− 0.5 V–1 V; step size: 10 mV; scan rate: 100 mVs^{-1}) which contains KCl (0.1 M) and $K_3[Fe(CN)_6]/K_4[Fe(CN)_6]$ (5mM, 1:1) solution as a redox probe. Electrochemical impedance measurements were carried out at 10.000 Hz–0.05 Hz frequency range. Square wave voltammetry measurements were performed in the potential range (− 0.2 V–0.7 V; frequency: 25 Hz; pulse size: 25 mV; equil. Time: 2 s). All electrochemical measurements were performed using a Gamry Potentiostat/Galvanostat, Reference 600 device at 25 °C.

All electrochemical measurements were performed in $K_3[Fe(CN)_6]/K_4[Fe(CN)_6]$ (5mM, 1:1) redox probe.

2.4. Human serum analysis of the TnT immunosensor

The TnT immunosensor was applied in real human serum samples. This study was performed by preparing three GP electrodes for different TnT concentrations (10 fg/mL and 100 fg/mL). These GP electrodes were prepared from the serum samples of 5 different individuals and the study were carried out by standard addition method. The standard addition method was performed by making necessary dilution procedures (1000 fold dilution) with phosphate buffer (0.05 M, pH 7.0) in accordance with the determination range of TnT in the human serum. The relative standard deviation (RSD) and the recovery values were calculated using equation obtained from the calibration graph of the immunosensor (Table 2).

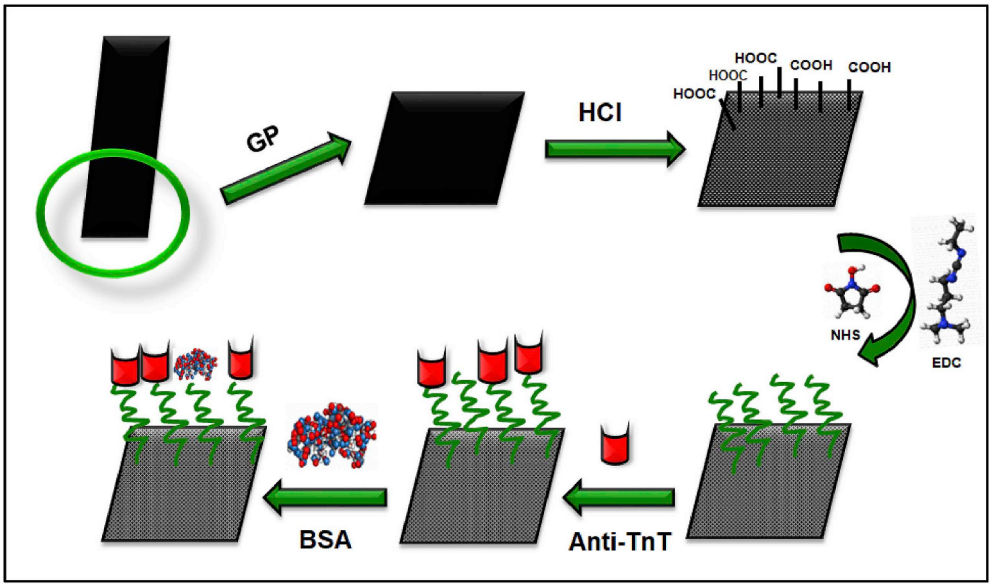

Scheme 1. The immobilization scheme of the proposed immunosensor.

Table 2
Determination of TnT biosensor in real serum samples.

Serum Number	TuT Concentration Value (fg/mL)	Standard Addition Value (fg/mL)	Measurement Conc. Value (fg/mL)	RSD (%) (n = 3)	Recovery (%)
1	30	10	39.56/38.56/39.16	1.56	97.5
		100	131.17/130.5/130.4	0.32	100.53
2	40	10	51.19/50.23/51.02	1.008	101.62
		100	140.08/140.15/141.2	0.45	100.34
3	50	10	60.1/62.4/59.06	2.82	100.86
		100	164.18/161.53/164.12	0.93	108.85
4	50	10	63.2/60.17/60.23	2.83	105.33
		100	169.02/159.1/163.2	3.04	109.18
5	30	10 100	42.02/44.11/40.01 141.4/131.9/136.2	4.87 2.55	105.12 105.00

3. Discussion and result

3.1. Electrochemical characterization of TnT immunosensor

The first step in creating the biosensor for the detection of the highly specific Troponin T (TnT) biomarker for acute myocardial infarction leading to cardiovascular disease is the cleaning process. Afterwards, HCl solution was used for the modification of the GP electrode surface. This process accelerated activation of carboxyl groups on the electrode surfaces. This activation was carried out by treating the GP electrode surface with acid solution, overnight. By this means, carboxyl groups on the surface were exposed by disturbing with the acid solution and the appropriate ambient conditions for the cross-linking agent EDC/NHS were achieved. Thus, the activated carboxyl groups allowed the GP electrode surface to become more suitable for immobilization. Then, the EDC/NHS pair which ensures the binding of anti-TnT to the surface was used. The immobilization of anti-TnT was achieved by this indispensable cross-linker EDC/NHS which allows the interaction between the functional carboxyl groups (-COOH) and the amine groups ($-NH_2$) [14]. Immediately after this step, anti-TnT incubation was performed to immobilize the antibody to the surface. In the final stage of immobilization, BSA blocking agent was used to prevent non-specific binding by closing the exposed functional groups. All these steps were followed with the EIS and CV techniques. When the EIS spectra in Fig. 1A is examined, the GP electrode measurement taken after the cleaning process had a very low signal. This situation indicates that the electrode surface underwent a successful cleaning stage, and in this way, risks due to any contamination that may form on the electrode surface were prevented. It also is a sign the conductivity in this stage is very high linked to this. The Rct value calculated from the EIS signal of the bare GP electrode is 17.81 Ω. The increase in EIS measurement after incubation in HCl solution proves that immobilization was successful with the calculated Rct (27.48 Ω) value of the chemical activations starting on the surface with acid treatment. Although the numerical difference between the values of Rct is not much, a highly conductive surface is negligible. Then, after cross-linking of EDC/NHS, the Rct value increased due to the increase in impedance signal and it was calculated as 40.97 Ω. The increased impedance signal with the immobilization of anti-TnT to the surface can be explained by the fact that the antibody inhibits diffusion by forming an insulating layer on the surface. The charge transfer resistance of the impedance signal of anti-TnT with a semicircular diameter was calculated to be 62.32 Ω. With BSA incubation, the diffusion of the analyte into the electrode surface, which has a high degree of insulation, became more difficult and this was reflected as an increase in the EIS spectrum. The Rct value of the BSA step was calculated as 99.12 Ω.

When the CV voltammograms in Fig. 1C are examined, the evaluations were made based on anodic and cathodic peak currents. First of all, the peak currents of the clean GP electrode taken after the cleaning process are quite smooth and sharp (cathodic peak current = 1.200 mA, anodic peak current = 1.242 mA). It was observed that the peak currents narrowed obviously in the CV measurement after HCl treatment (cathodic peak current = 660.0 μA, anodic peak current = 809.3 μA). After incubation of EDC/NHS, the peak currents were closer to each other as seen in this voltammogram due to the fact that the redox probe could not diffuse to the electrode surface (cathodic

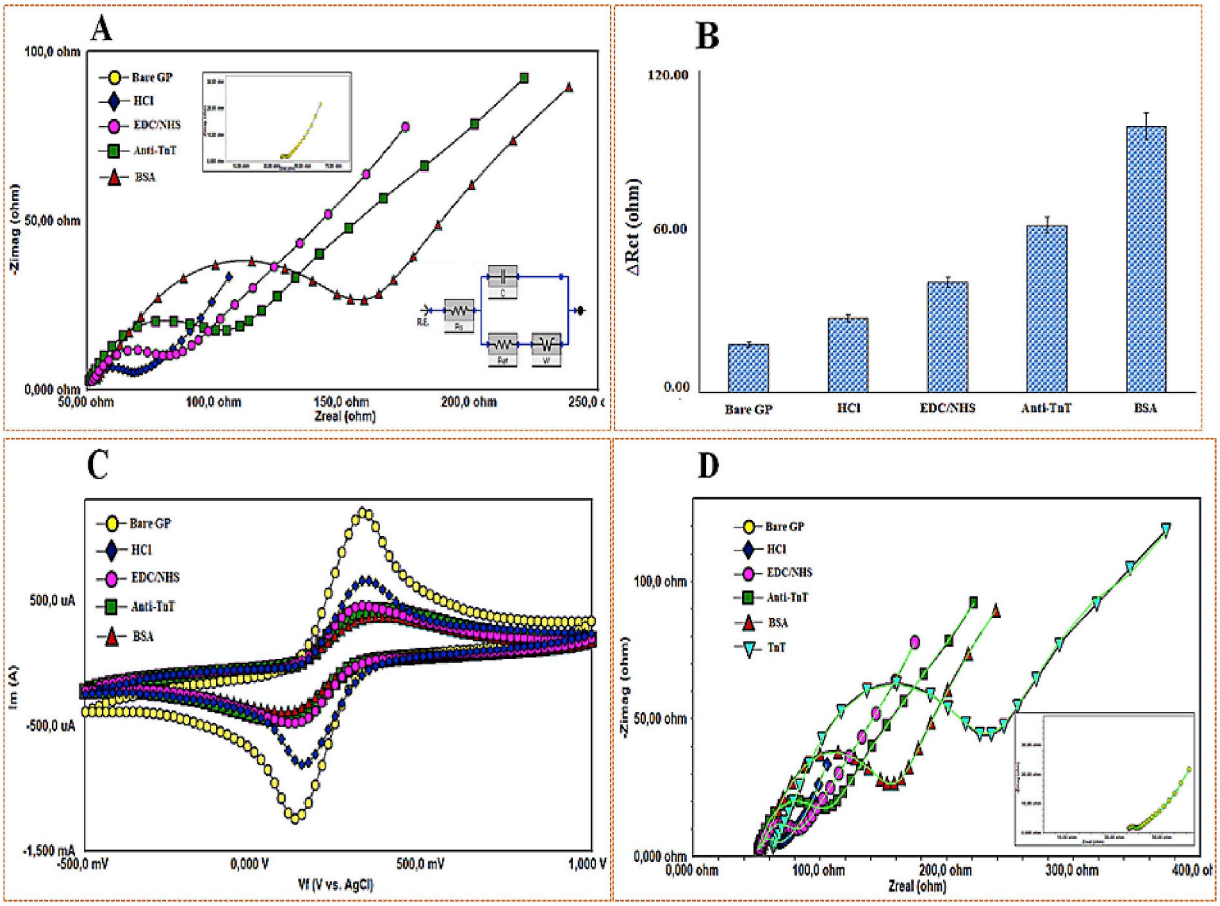

Fig. 1. EIS spectra (A), Rct values (B) CV voltammograms (C) of the TnT immunosensor and Kramer's Kronig Tranform (D).

peak current = 456.5 μA, anodic peak current = 480 μA). With increasing immobilization of anti-TnT, peak currents decreased further with increasing insulation (cathodic peak current = 422.6 μA, anodic peak current = 448.8 μA). Finally, with the incubation of BSA, the immobilization stage (cathodic peak current = 365.1 μA, anodic peak current = 387.9 μA) with the lowest peak current values occurred due to the inhibition of surface diffusion which caused further insulation.

The EIS spectra for immobilization of the TnT biosensor, the Rct values and CV voltammograms of each step are given in Fig. 1.

3.2. Morphological characterization of TnT immunosensor

The surface morphology of the TnT biosensor after immobilization steps was examined with the scanning electron microscope technique. The SEM images of the biosensor are given in Fig. 2. First, the SEM image seen in Fig. 2A belongs to the GP electrode surface after the cleaning step. The surface with no immobilization was displayed as a flat sheet. In Fig. 2B, the SEM image was taken after the treatment of the electrode surface with HCl. The surface change after acid treatment is clearly seen compared to the SEM image of the previous clean electrode surface. In Fig. 2C, after the immobilization of the EDC/NHS pair used to activate the carboxyl groups, the SEM images have more intense groups on the surface. Fig. 2D is an SEM image showing the change in surface morphology with covalent bonding of anti-TnT to the GP electrode surface. When the image is examined, there are structures that are very densely stacked on the surface. In Fig. 2E, there is an SEM image taken after immobilization of BSA used to avoid non-specific interactions. Finally, in Fig. 2F, there is an SEM image of the morphological change of the surface with the incubation of TnT. In this image, the objects on the surface resemble a stone.

3.3. Optimization studies of TnT immunosensor

In order to determine the optimum value of HCl acid concentration, which has a critical role in the immobilization of the surface, an optimization study was carried out with great care. This step is very crucial to disturb the carboxyl groups on GP electrode surface which has very stable carbon surface and to carry out a successful immobilization process. Therefore, it is necessary to determine the optimum acid concentration carefully to avoid damaging the surface and to obtain a stable immobilization surface. In this optimization study, the effect of HCl acid on the biosensor was investigated with 4 different concentration values (1 M, 1.5 M, 3 M and 6.25 M). For this purpose, EIS and CV measurements were taken with the biosensor prepared with 1 M HCl starting from low concentration values first. In this optimization step, the other parameters such as antibody concentration, antibody incubation time and TnT incubation time were kept as 13 ng mL-1, 45 min and 30 min respectively. When the data obtained from the measurements are examined, it is thought that the immobilization of the surface cannot be completed in the low acid concentration. The impedance signals, which are very close to each other during the operation, reinforce this possibility. Therefore, the next concentration was chosen as 1.5 M HCl and the biosensor was prepared at this concentration. When the standard curve in Fig. 3A, which is generated by the Rct values calculated from the EIS signals, is examined, it appears to have higher signals than the previous concentration. The next HCl concentration was chosen as 3 M. At the end of the study, it is clearly seen that there is an increase in the signals of the standard curve with increasing concentration. The final preference concentration value for optimization was determined as 6.25 M HCl. This concentration value with the highest signal is considered to be the optimum HCl

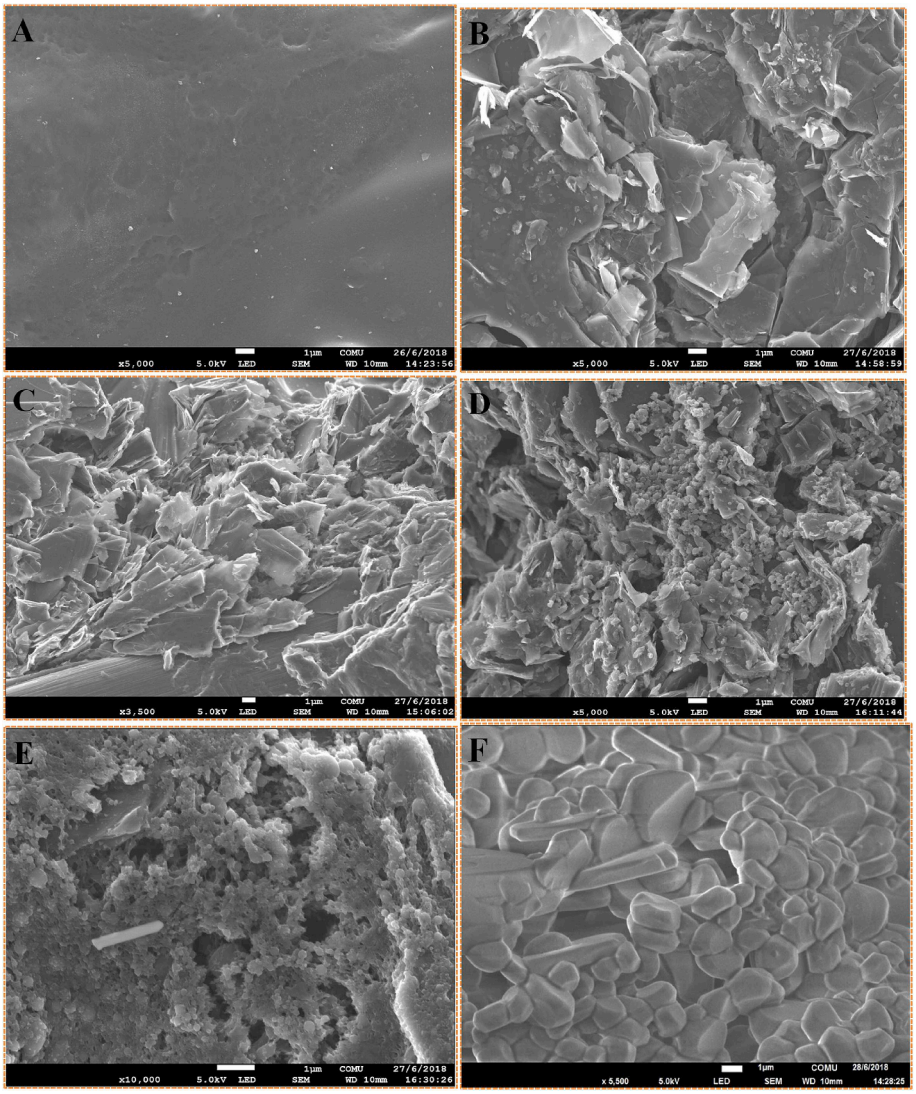

Fig. 2. SEM images of the TnT immunosensor. (A) bare GP, (B) HCl, (C) EDC-NHS, (D) Anti-TnT, (E) BSA, (F) TnT.

concentration. At concentrations of more than 6.25 M HCl, studies at higher concentrations could not be carried out as the electrode surface became severely damaged by intensive acid treatment and immobilization became impossible. Standard graphics for HCl concentration optimization are given in Fig. 3A.

An optimization study was performed at 3 different concentrations (6.5 ng/mL, 13 ng/mL and 26.6 ng/mL) to investigate the effect of anti-TnT on the developed biosensor response. First, the biosensor was prepared with 6.5 ng/mL anti-TnT concentration and monitored by EIS and CV measurements. The data obtained form a standard curve with smooth signals in the study. However, in order to investigate the effect of the biosensor on higher antibody concentrations, further optimization procedures were continued with more concentrated anti-TnT concentrations. Therefore, another study was performed with 13 ng/mL of anti-TnT. When the standard curve obtained at the end of the study is examined, the signal with 6.5 ng/mL is clearly different. Based on these results, it was determined that the increase in the signal due to the charge transfer resistance is also affected by the immobilization of the biosensor. The next concentration was 26.6 ng/mL. When the results of the study for the selected concentration were examined, a decrease was observed in EIS signals in contrast to what was expected. The reason for this is that the decrease in activity of the anti-TnT antibody when it reaches saturation on the surface is thought to be due to a signal drop. In this optimization step, the other parameters such as HCl concentration, antibody incubation time and TnT incubation time were kept as 6.25 M, 45 min and 30 min respectively. For all these reasons, the optimum anti-TnT concentration was determined as 13 ng/mL. Standard graphics for anti-TnT concentration optimization are given in Fig. 3B.

After the optimum concentration value of the anti-TnT antibody was determined, an optimization study was carried out to determine the incubation time on the electrode surface. Biosensors were prepared in 3 different periods (30, 45 and 60 min) and followed with EIS and CV measurements. In accordance with the data obtained from the studies conducted separately for each period, standard graphics of the biosensors given in Fig. 3C were generated and compared with each other. When the standard curves are examined, the lowest signals belong to the incubation period of 45 min. For incubation periods of 60 and 30 min, the signals are very close to each other. For this reason, the optimum anti-TnT incubation time was chosen as 30 min considering time saving for the practicality of the designed biosensor. In this optimization step, the other parameters such as HCl concentration, antibody concentration and TnT incubation time were kept as 6.25 M, 13 ng/mL and 30 min respectively.

The final optimization study of the developed biosensor is to determine the incubation time for the TnT biomarker. For this study, 3 different times (30, 45 and 60 min) were studied and EIS and CV measurements were taken. As a result of the calculations made with the

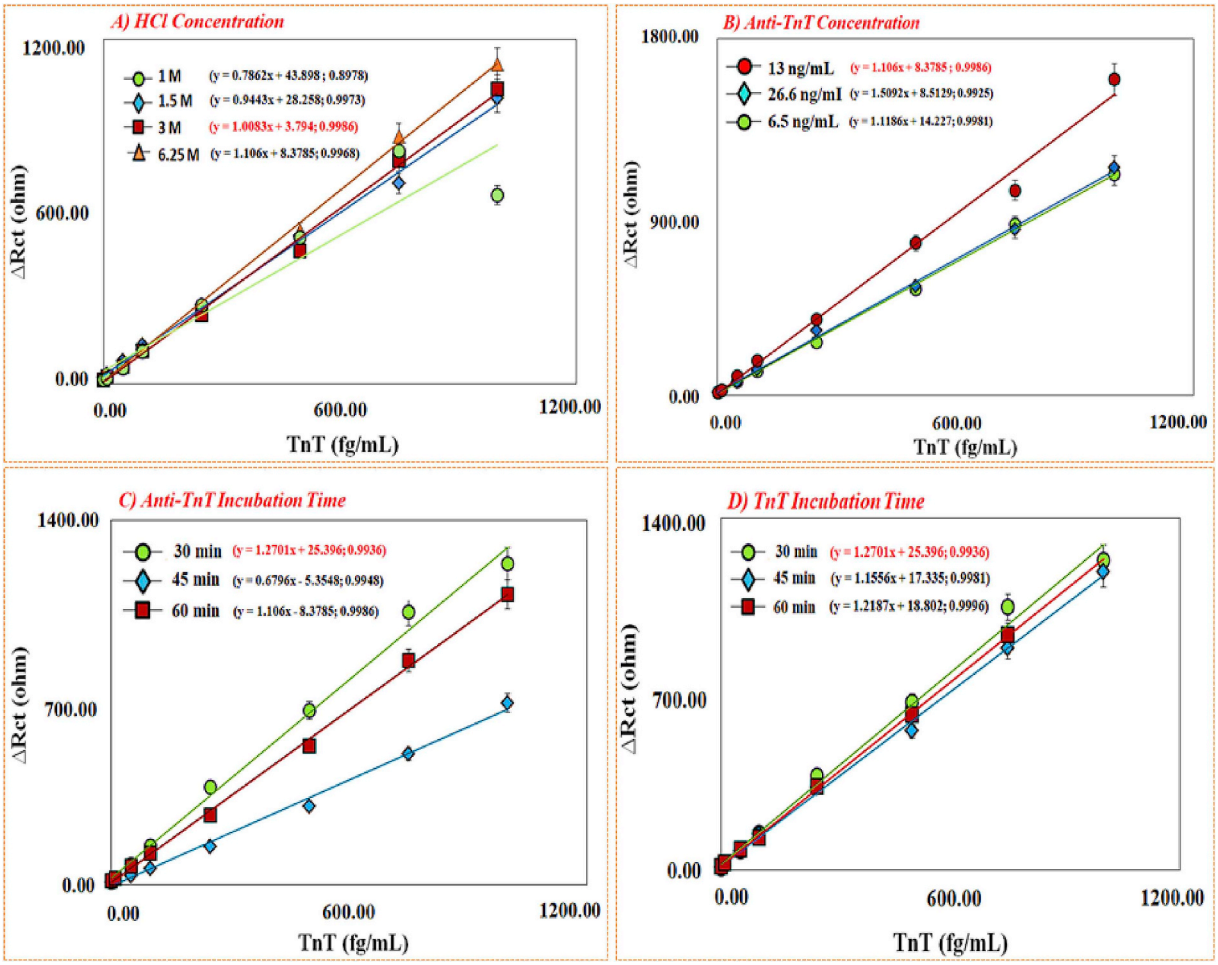

Fig. 3. Optimization linear graphs of the TnT biosensor A) HCl concentration, B) Anti-TnT Concentration; C) Anti-TnT Incubation Time, D) TnT Incubation Time.

Rct values obtained from the EIS data of the biosensors, the standard graphs in Fig. 3D were generated. When the standard curves of the biosensors are examined, the results are almost coincident with each other in the 3 studies. According to these results, the designed biosensor had 30 min selected as the optimum incubation time for the TnT biomarker, which highlights its practicality due to preparation in a short time. In this optimization step, the other parameters such as HCl concentration, antibody concentration and anti-TnT incubation time were kept as 6.25 M, 13 ng/mL and 30 min respectively.

3.4. Analytical studies of TnT immunosensor

After all optimization procedures were completed, the TnT biomarker prepared at increasing concentrations of the developed biosensor was determined by EIS and CV techniques. In this study, which was carried out by determining 8 different concentration values, a linear range for precise TnT determination by the developed biosensor was determined. The design of the sensor was determined as 0.5–1000 fg/mL. The developed immunosensor can perform TnT analysis at a very high concentration level in a wide range, such as the femtogram. The calibration graph of the TnT biosensor, the EIS spectrum of this calibration graph, and the CV voltammogram is given in Fig. 4. The LOD and LOQ values were also calculated as 1.28 fg/mL and 4.29 fg/mL, respectively. Impedimetric data of TnT at increased concentrations are given in Table 3.

For the repeatability study of the TnT biosensor, 20 different electrodes were prepared under the same conditions and incubated with TnT at the same concentration (50 fg/mL) to obtain EIS measurements. The Rct values obtained from the EIS measurements of each electrode are taken from the biosensor using the calibration equation shown in Fig. 4C with average value of 50.3625 fg/mL, standard deviation value 1.045 fg/mL and the variation coefficient was calculated as 2.07%.

The electrodes prepared under optimum conditions were studied in different time periods for the reproducibility study of the proposed immunosensor. Ten biosensors were prepared for this study, which was performed by measuring the determination range determined by increasing concentrations of TnT. Standard graphs of each biosensor were obtained and compared with each other from the Rct values in the EIS data of the prepared biosensors. In addition, relative standard deviations of slope and intercept values were calculated as 2.98% and 5.87%, respectively, within the reproducibility of the biosensor. The reproducibility results of the TnT biosensor are shown in Fig. 4D.

In the characterization studies of the designed biosensor, a reusability study was conducted to examine the stability of the electrode surface and also to reduce the cost of the biosensor in routine use. This study was performed by removing the bound protein from the surface by keeping the TnT-bound electrode surface in 10 mM HCl acid solution for 5 min. After this procedure, EIS was measured by incubating TnT (50 fg/mL) at a certain concentration on the same surface again. This process continued until the protein's ability to bind the protein to a high extent was partly or completely lost. For the TnT biosensor, this was done 20 times. At the 17th repetition, it was able to carry out the determination of TnT by maintaining the majority of its activity until binding. However, the transaction ended when the biosensor lost most of its activity at the 20th binding. These reusability results for the TnT biosensor designed with electrodes are quite good. This superiority,

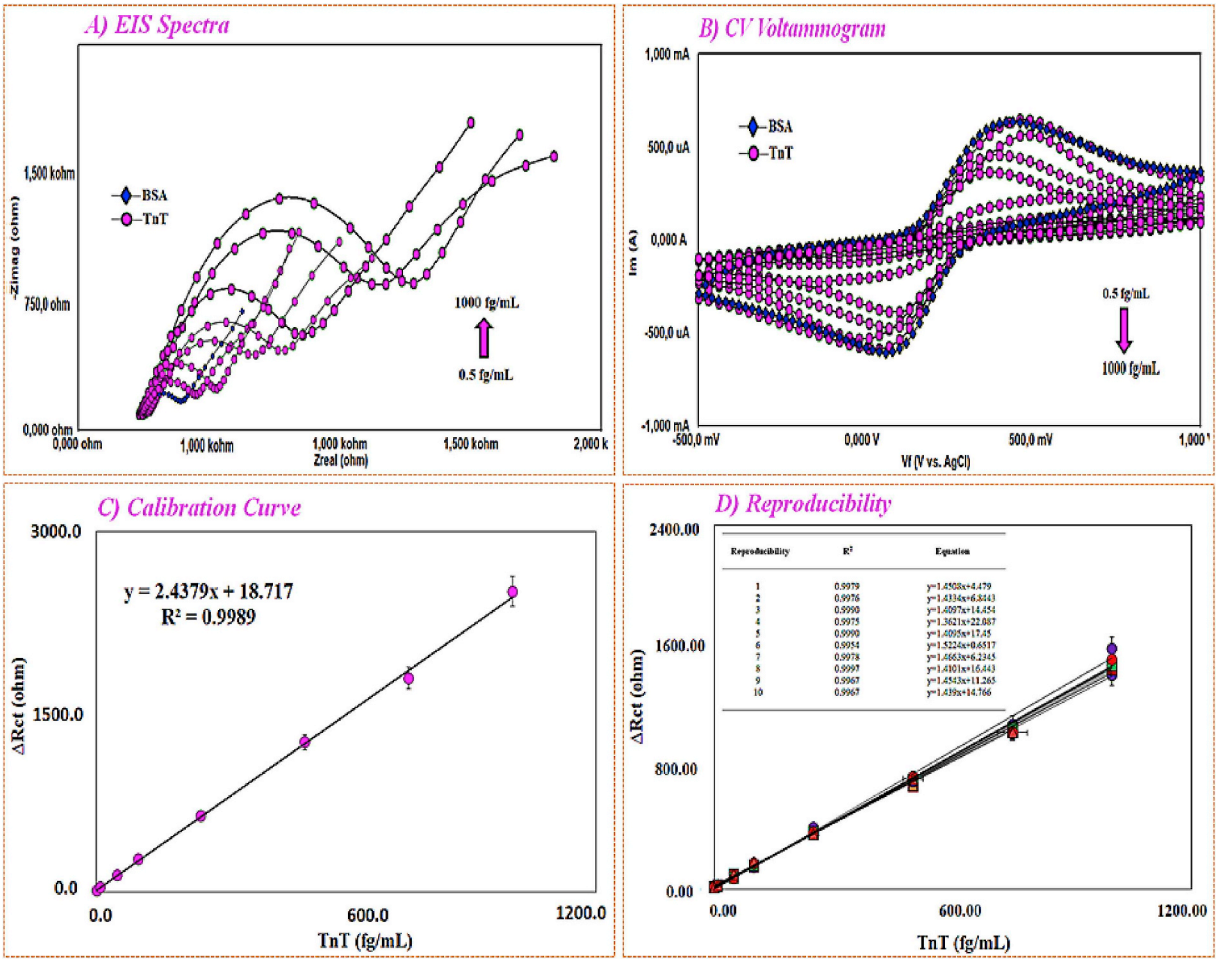

Fig. 4. The detection of the TnT at increased concentrations A) EIS spectra, B) CV voltammograms, C) Calibration Curve (0.5–1000 fg/mL), D) Reproducibility.

which can provide an advantage with significant differences in the cost of the biosensor, is also a feature sought for clinical applications. The graph of the TnT biosensor reusability study is given in Fig. 5A.

For the TnT biosensor designed with a fixed frequency impedance technique, it is possible to examine the kinetic binding between anti-TnT and TnT. The fixed frequency value determined from the Bode graph in Fig. 5C(A) was measured as the function of time and phase angle at 45.07 Hz. The constant frequency time-dependent impedance changes of the TnT biosensor are shown in Fig. 5C(B). Fig. 5C(B) illustrates the impedance measurement taken at a fixed frequency with the pink curve, while the blue curve represents the phase angle measurements. In this process, which takes place in pH 7.0 phosphate buffer, it is clear that the TnT biomarker is connected with time. The measurement is completed by reaching the saturation point of TnT around 1000 ks (17 min).

In addition to EIS and CV techniques, the developed biosensor was also determined with square wave voltammetry. The SWV frequency for this run is selected as 25 Hz, the potential range is −0.2/0.7 V, and increasing concentrations of TnT were measured. The following equation was used to calculate the measurements.

$$\Delta Idif = \Delta Idef(BSA) - \Delta Idif(TnT)$$

Fig. 5D shows the square wave voltammograms and calibration graphs of the TnT measurement in the detection range of 0.5 f g to 1000 fg/mL at optimum conditions.

The surface coverage study was carried out by using the Laviron equation ($Q = nxFxAx\Gamma$; n:slope, F: Faraday constant (96485C mol^{-1}), A: Electrode surface area (cm^2), Q: Charge (C) and Γ: Coated surface area (mol/cm^2)) for the analytical studies of the proposed immunosensor. In order to perform this work, the voltammetric technique was used and the GP electrode surface was scanned at ten different speed values in each immobilization step. These speed values were 10, 20, 30, 40, 50, 60, 70, 80, 90 and 100 mV s^{-1}, respectively. Using the peak currents obtained from the cyclic voltammograms, the calculated data were substituted in the Laviron equation and the surface area of the GP electrode was calculated. When the results were evaluated, the GP surface initially calculated to be 1.5×10^{-8} mol cm^{-2}, was calculated to be 3.7×10^{-8} mol cm^{-2} after anti-TnT binding. This result indicated that anti-TnT was immobilized onto the surface.

The proposed immunosensor exhibited long storage stability. This is a feature that will enable both the stability of the sensor developed and its preference in clinical applications. In order to determine the shelf life of the developed sensor, the sensors with immobilization procedures were stored at + 4 °C until TnT was determined. EIS was measured after TnT incubation at a determined concentration (50 fg/mL) within the assay interval for a total of 7 weeks, including a sensor each week. The Rct values obtained from the measurements taken were taken into consideration in the calibration graph equation in Fig. 5B and calculations were made. Fig. 5B shows the 7-week performance of the TnT biosensor for storage stability. It is observed that the biosensor designed in the graph maintains a high level of activity for 5 weeks and this activity decreases slightly in the 6th and 7th weeks. The total activity loss during the 7-week period of the TnT biosensor designed with chemical modification was calculated as 20.84%. The shelf life of the biosensor, which corresponds to approximately 50 days in total, is also suitable for practical applications.

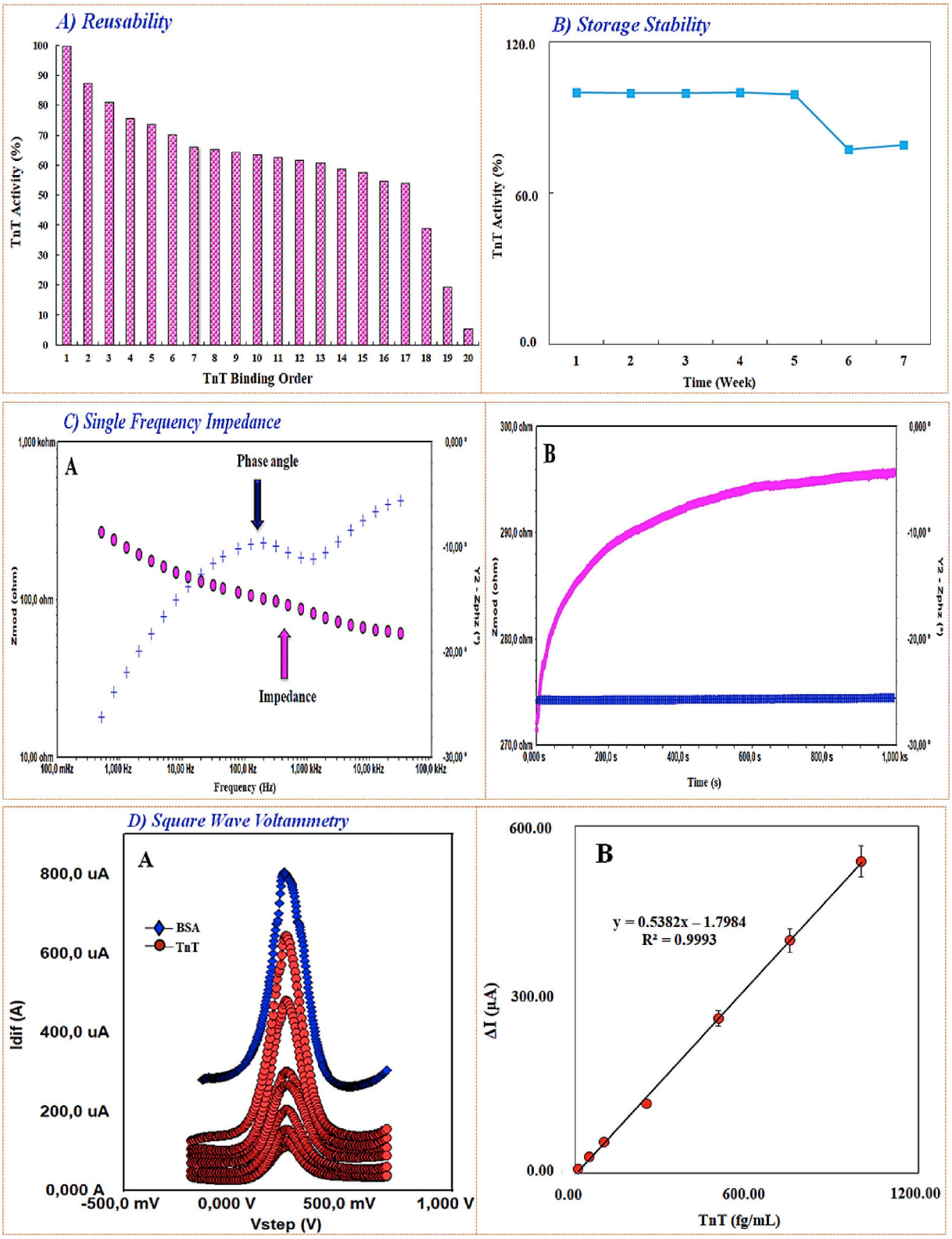

Fig. 5. Analytical Studies of the TnT immunosensor A) Reusability, B) Storage Stability C)Single Frequency Impedance Analysis ((A) Bode plot, (B) SFI Analysis); D) SWV Analysis ((A) SWV Voltammogram, (B) Calibration Curve of SWV Analysis)).

In order to examine the usability of the developed biosensor for clinical applications, TnT was determined by the standard addition method in human serum samples from different individuals. The EIS data were obtained by adding different concentrations of TnT (10 fg/mL and 100 fg/mL) to the serum samples. For this data, relative standard deviation (RSD) and recovery percentages were calculated for each serum using the equation for the calibration graph. The results of the calculations made with serum samples are given in Table 2.

The Kramers-Kronig transform is a method used to examine whether the designed biosensor is affected by any external factors during EIS

Table 3
Depending on the increased TnT concentration, the Rct, Ru and C_{dl}.

Electrode	Rct(olun)	Ru (olun)	C_{dl}(μF)
TnT Biosensor	56.24 ± 0.8977	59.97 ± 0.5128	5.48 ± 0.224
TnT 0.5 fg/mL	77.77 ± 1.002	59.62 ± 0.47	9.033 ± 0.2875
TnT 10 fg/mL	102.7 ± 1.132	56.26 ± 0.4437	S.039 ± 0.205 S
TnT 50 fg/mL	161.9 ± 1.719	69.66 ± 0.51	12.5 ± 0.2795
TnT 100 fg/mL	189.3 ± 1.871	71.55 ± 0.527	10.62 ± 0.2206
TnT 250 fg/mL	352.9 ± 3.491	147.9 ± 1.149	3.157 ± 0.07
TnT 500 fg/mL	700.0 ± 6.782	280.5 ± 2.3 63	0.8061 ± 0.01715
TnT 750 fg/mL	936.9 ± 8.829	299.8 ± 2.45	0.9277 ± 0.0177
TnT 1000 fg/mL	1010 ± 9.56	300.5 ± 2.424	0.9419 ± 0.01766

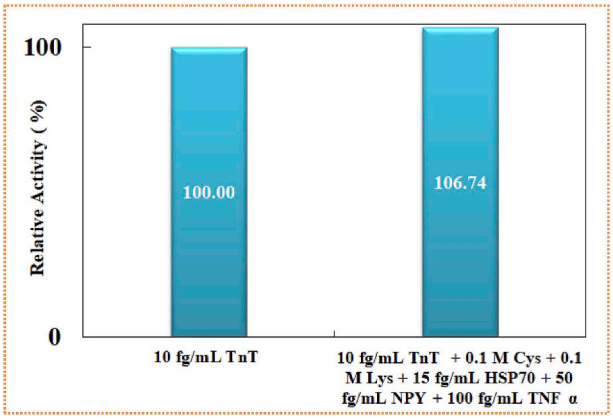

Fig. 6. Selectivity study of the TnT immunosensor.

measurements and, accordingly, deviations [25,26]. For the immobilization stages of the TnT biosensor, the impedance spectra are shown in Fig. 1D.

The selectivity study for target TnT was performed for the proposed immunosensor to understand either there is non-specific interactions or interferences. For this aim, two electrodes were prepared under optimum conditions for the proposed immunosensor. The first electrode was only treated with TnT solution (10 fg/mL). The other electrode was treated with the solution including TnT solution (10 fg/mL), cysteine solution (0.1 M), lysine solution (0.1 M), heat shock protein 70 solution (15 fg/mL), neuropeptide Y solution (50 fg/mL), tumor necrosis factor α solution (100 fg/mL). The obtained ΔRct values from the immunosensor responses were compared with each other the results are seen in Fig. 6. As clearly seen in the figure, the developed immunosensor successfully showed a high selectivity capacity for target TnT.

4. Conclusion

The determination of TnT, the specific biomarker of acute myocardial infarction, is very important. For this reason, there are many sensors in the literature to perform this important biomarker analysis. However, these sensors are often produced with more expensive techniques and with lower precision. GP electrode has a lot of advantages such as carbon surface suitable for practical immobilization, low cost (about 0.15 $ for the proposed immunosensor), surface stability compared to another working electrode used in many biosensors in the literature (e.g. gold electrode, carbon paste electrode, screen printed electrode, etc.).

As can be seen from the results obtained from the regeneration study (Fig. 5A), this electrode had a very stable surface and allowed a stable and practical immobilization.

The TnT biosensor system developed in this study was created using very practical electrochemical methods such as EIS and CV with low cost electrodes such as disposable GP, and a very practical immobilization procedure. In addition, this sensor system, which enables TnT analysis in a wide detection range of 0.5–1000 fg/mL, also yielded promising results after studies in human serum. The proposed immunosensor could determine the TnT antigen at sub-femtogram concentrations.

Novelty statement

TnT immunosensor being prepared without the need for any cross-linking agent due to the HCl acid, has a wide detection range (0.5 – 1000 fg/mL). The human serum study showed that the proposed biosensor could correctly analyze detection of TnT with low-cost disposable graphite paper electrodes instead of expensive methods like ELISA test.

References

[1] http://www.who.int/mediacentre/factsheets/fs317/en/ , Accessed date: 17 August 2016.
[2] E. Giannitsis, K. Kurz, K. Hallermayer, J. Jarausch, A.S. Jaffe, et al., Analytical validation of a high-sensitivity cardiac troponin T assay, Clin. Chem. 56 (2010) 254–261.
[3] E.B. Bahadır, M.K. Sezgintürk, Applications of electrochemical immunosensors for early clinical diagnostics, Talanta 132 (2015) 162–174.
[4] M. De Antonio, J. Lupón, A. Galán, J. Vila, E. Zamora, A. Urrutia, C. Díez, R. Coll, S. Altimir, A. Bayes-Genis, Head-to-head comparison of high-sensitivity troponin T and sensitive-contemporary troponin I regarding heart failure risk stratification, Clin. Chim. Acta 426 (2013) 18–24.
[5] N. Zanato, L. Talamini, E. Zapp, D. Brondani, I.C. Vieira, Label-free electrochemical immunosensor for cardiac troponin T based on exfoliated graphite nanoplatelets decorated with gold nanoparticles, Electroanalysis 29 (2017) 1820–1827.
[6] K. Thygesen, J.S. Alpert, Myocardial infarction redefined–a consensus document of the Joint European Society of Cardiology/American College of Cardiology Committee for the redefinition of myocardial infarction, J. Am. Coll. Cardiol. 36 (2000) 959–969.
[7] J.L. McDonough, J.E. Van Eyk, Developing the next generation of cardiac markers: disease-induced modifications of troponin I, Prog. Cardiovasc. Dis. 47 (2004) 207–216.
[8] X. Dai, R.G. Compton, Direct Eelectrode position of gold nanoparticles onto indium tin oxide film coated glass: application to the detection of Arsenic(III), Anal. Sci. 22 (2006) 567.
[9] Y.T. Ma, J.W. Di, X. Yan, M.L. Zhao, ZhJ. Lu, Y.F. Tu, Direct electrodeposition of gold nanoparticles on indium tin oxide surface and its application, Biosens. Bioelectron. 24 (2009) 1480.
[10] D.W. Wang, F. Li, J.P. Zhao, W.C. Ren, Z.G. Chen, J. Tan, Z.S. Wu, I. Gentle, G.Q. Lu, H.M. Cheng, Fabrication of graphene/polyaniline composite paper via in situ anodic electropolymerization for high-performance flexible electrode, ACS Nano 3 (2009) 1745.
[11] W.H. Cai, T. Lai, H.J. Du, J.S. Ye, Electrochemical determination of ascorbic acid, dopamine and uricacid based on an exfoliated graphite paper electrode: a high performance flexible sensor, Sens. Actuators, B 193 (2014) 492.
[12] J. Kariuki, E. Ervin, C. Olafson, Development of a Novel Low-Cost, Disposable wooden pencil graphite electrode for use in the determination of antioxidants and other biological compounds, Sensors 15 (2015) 18887.
[13] E. Alipour, M.R. Majidi, A. Saadatirad, S.M. Golabi, A.M. Alizadeh, Simultaneous determination of dopamine and uric acid in biological samples on the pretreated pencil graphite electrode, Electrochim. Acta 91 (2013) 36.
[14] E.Y. Liu, S. Jung, H. Yi, Improved protein conjugation with uniform, macroporous poly(acrylamide-co-acrylic acid) hydrogel microspheres via EDC/NHS chemistry, Langmuir 32 (2016) 11043–11054.
[15] Y. Han, H. Kim, Y. Park, H. Chun, J. Kim, H. Yoon, Retroreflective Janus microparticle as a nonspectroscopic optical immunosensing probe, ACS Appl. Mater. Interfaces 8 (2016) 10767–10774.
[16] H. Jo, H. Gu, W. Jeon, H. Youn, J. Her, S. Kim, J. Lee, J.n. Shi, C. Ban, Electrochemical aptasensor of cardiac troponin i for the early diagnosis of acute myocardial infarction, Anal. Chem. 87 (2015) 9869–9875.
[17] W. Zhao, R. Chen, P. Dai, X. Li, J. Xu, H. Chen, A general strategy for photoelectrochemical immunoassay using an enzyme label combined with a CdS quantum dot/TiO2 nanoparticle composite electrode, Anal. Chem. 86 (2014) 11513–11516.
[18] Y. Liu, L. Yobas, Label-free specific detection of femtomolar cardiac troponin using an integrated nanoslit array fluidic diode, Nano Lett. 14 (2014) 6983–6990.
[19] T.M. Jiang, P. Lu, Y.-M. Lei, Y.-Q. Chai, R. Yuan, Y. Zhuo, Self-accelerated electrochemiluminescence emitters of Ag@SnO2 nanoflowers for sensitive detection of cardiac troponin T, Electrochim. Acta 271 (2018) 464–471.
[20] M. Karimi, M. Rabiee, M. Tahriri, R. Salarian, L. Tayebi, A graphene based–biomimetic molecularly imprinted polyaniline sensor for ultrasensitive detection of human cardiac troponin T (cTnT), Synth. Met. 256 (2019) 116136.
[21] L. Wang, M. Xu, R. Huang, X. Chang, C. Chen, L. Li, Z. Zhang, Y. Han, A dual-label time-resolved fluorescence immunoassay for the simultaneous determination of cardiac troponin T and myoglobin, SLAS Technol. 22 (2017) 130–135.

[22] M. Negahdary, M. Behjati-Ardakani, H. Heli, An electrochemical troponin T aptasensor based on the use of a macroporous gold nanostructure, Microchimica Acta 186 (2019) 377.
[23] M.L. Yola, N. Atar, Development of cardiac troponin-I biosensor based on boron nitride quantum dots including molecularly imprinted polymer, Biosens. Bioelectron. 126 (2019) 418–424.
[24] K. Phonklam, R. Wannapob, W. Sriwimol, P. Thavarungkul, T. Phairatana, A novel molecularly imprinted polymer PMB/MWCNTs sensor for highly-sensitive cardiac troponin T detection, Sensor. Actuator. B 308 (2019) 127630, https://doi.org/10.1016/j.snb.2019.127630.
[25] B. Özcan, B. Demirbakan, Ş.G. Yeşiller, M.K. Sezgintürk, Introducing a new method for evaluation of the interaction between an antigen and an antibody: single frequency impedance analysis for biosensing systems, Talanta 125 (2014) 7–13.
[26] B. Demirbakan, M.K. Sezginturk, A sensitive and disposable indium tin oxide based electrochemical immunosensor for label-free detection of MAGE-1, Talanta 169 (2017) 163–169.